Journal of
Materials Chemistry A

Accepted Manuscript

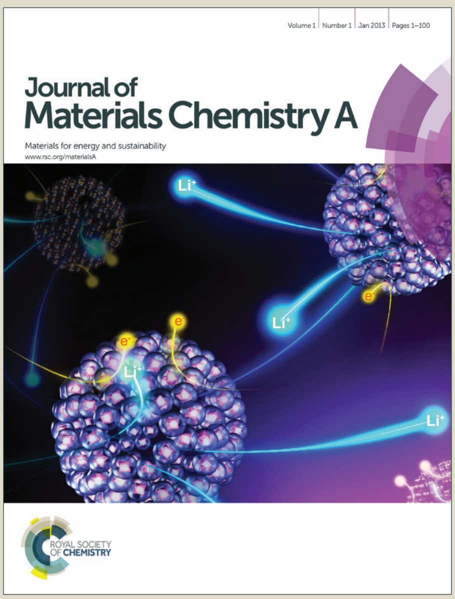

This is an *Accepted Manuscript*, which has been through the Royal Society of Chemistry peer review process and has been accepted for publication.

Accepted Manuscripts are published online shortly after acceptance, before technical editing, formatting and proof reading. Using this free service, authors can make their results available to the community, in citable form, before we publish the edited article. We will replace this *Accepted Manuscript* with the edited and formatted *Advance Article* as soon as it is available.

You can find more information about *Accepted Manuscripts* in the Information for Authors.

Please note that technical editing may introduce minor changes to the text and/or graphics, which may alter content. The journal's standard Terms & Conditions and the Ethical guidelines still apply. In no event shall the Royal Society of Chemistry be held responsible for any errors or omissions in this *Accepted Manuscript* or any consequences arising from the use of any information it contains.

ROYAL SOCIETY OF CHEMISTRY

www.rsc.org/materialsA

Journal Name

Dynamic Article Links ►

Cite this: DOI: 10.1039/c0xx00000x

www.rsc.org/xxxxxx

ARTICLE TYPE

Core-Shell Co@C catalyzed MgH_2: Enhanced dehydrogenation properties and its catalytic mechanism

Ying Wang,[a] Cuihua An,[a] Yijing Wang[*a], Yanan Huang,[a] Chengcheng Chen,[a] Lifang Jiao,[a] Huatang Yuan[a]

Received (in XXX, XXX) Xth XXXXXXXXX 20XX, Accepted Xth XXXXXXXXX 20XX
DOI: 10.1039/b000000x

An efficient core-shell Co@C catalyst is synthesized through a solvothermal and subsequent annealing process. The as-synthesized Co@C is consisted of 11 nm Co core and 3 nm amorphous carbon shell. Nitrogen sorption isothermals show that Co@C has a surface area of 112.6 $m^2\ g^{-1}$ and a typical pore size of 4.8 nm. The catalytic effects of core-shell Co@C are systematically investigated, which can significantly improve the dehydrogenation performances of MgH_2. With the increasing amount of Co@C (0, 3, 5, 10, 15 wt%), the dehydrogenation temperature of MgH_2 decreased . Its dehydrogenation kinetics is also improved, especially, the MgH_2-10%Co@C sample starts to release hydrogen at 168 ^oC, about 6.00 wt% hydrogen is released during its decomposition. The activation energy of MgH_2-10%Co@C is determined to be 84.5 kJ mol^{-1}, 46.2 % decreased than that of pure MgH_2. Mechanism analysis indicates that upon increasing the Co@C content the decomposition of MgH_2 gradually happens along lower-dimensional nucleation and growth. Moreover, the super thermal conductivity of carbon shell in Co@C also makes contribution to the enhanced dehydrogenation performances of MgH_2.

Introduction

Hydrogen, the lightest element on the earth, has a high energy efficiency of 142 MJ kg^{-1} and it is clean and renewable. So hydrogen is expected to play a vital role in the future energy system.[1, 2] For practical usage, the hydrogen storage mediums must be light, high density and affordable. MgH_2 has potential to meet these requirements. Generally, the de/re-hydrogenation of MgH_2 is expressed as following:

$$MgH_{2(s)} \underset{rehydrogen}{\overset{dehydrogen}{\rightleftarrows}} Mg_{(s)} + H_{2(g)} \qquad (1)$$

The theoretical hydrogen storage capacity of MgH_2 is 7.6 wt% (110 kg m^{-3}), large enough to satisfy the target of DOE. However, the commercial applications of MgH_2 are still suffer from sluggish de/re-hydrogenation kinetics and high thermodynamic stability. The tough thermal management of MgH_2 has also arisen much research attention.[3-5] Therefore, a proper way is needed to solve these drawbacks and make MgH_2 promising for both stationary and on-board energy storage. In practice, adding transition metals (TMs) is an effective strategy to modify the hydrogen storage properties of MgH_2.[6] For example, Hanada et al.[7] found that TMs catalyzed MgH_2 showed better hydrogen desorption properties than pure MgH_2. A comparative study about the stability of MgH_2:Ti and MgH_2:Co was performed by Novakovic´ et al.,[8] which declared that the higher number of d-electrons in Co metal made it more pronounced than Ti in destabilizing MgH_2. Other experiments also confirmed the favorable effects of Co on MgH_2. However, most of them concerned just about bulk or irregular Co powders.[9-12]

It is well known that same material can display obvious different performance, depending on its morphology and microstructure.[13-17] Generally, the core-shell structure shows improved physical and chemical properties than their bulk competitors.[18-21] The unique nature of core-shell structure has led to numerous new applications in chemistry, bioscience and material science. In our previous work,[22] 1D nanorod structured Co@C, which was assembled by plenty of core-shell particles, was successfully synthesized and used as negative material for alkaline secondary batteries. Taking the unique structure of Co@C into consideration, it is expected to exhibit enhanced catalytic effects on the dehydrogenation properties of MgH_2.

In this work, we studied the catalytic effects of core-shell Co@C on the dehydrogenation performances of MgH_2. To gain more insight in the effects of doping amount, different weight ratio of Co@C (0, 3, 5, 10, 15 wt%) is added to MgH_2. The dehydrogenation performances of as-prepared MgH_2-Co@C composites are systematically investigated. Compared with pure MgH_2, the addition of Co@C remarkably enhanced the desorption properties of MgH_2 which can be explained from the point of kinetics modification. The catalytic mechanism of Co@C is explored by using the Johnson-Mehl-Avrami modeling, X-ray diffraction and X-ray photoelectron spectrometer.

Experimental

Synthesis of core-shell Co@C

Journal of Materials Chemistry A Accepted Manuscript

This journal is © The Royal Society of Chemistry [year]

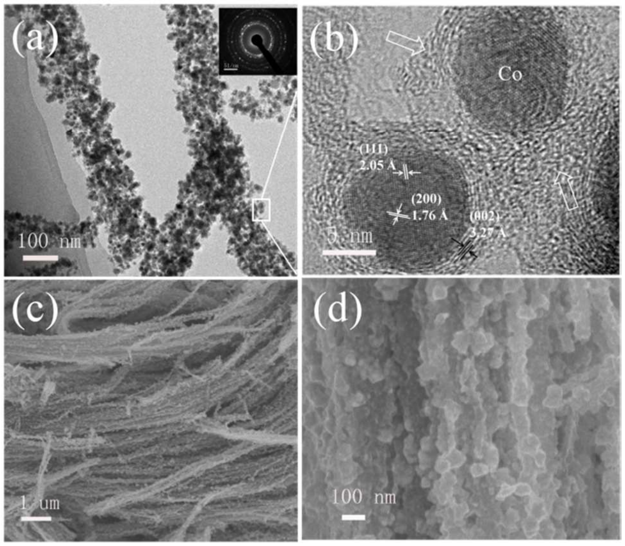

Fig.1 (a) TEM, (b) HRTEM and (c-d) SEM images in different resolution of the as-prepared Co@C sample. Insert (a) is the SAED pattern.

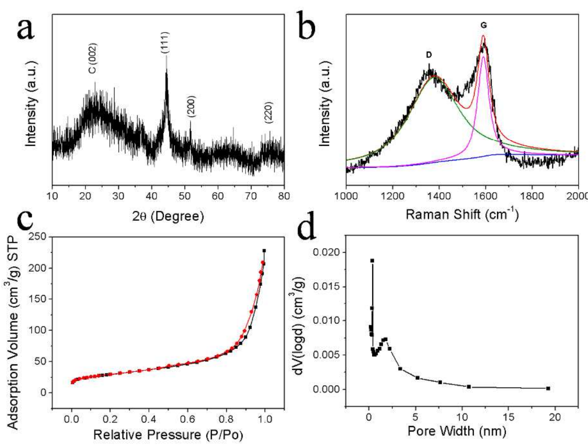

Fig.2 (a) XRD, (b) Raman, (c) nitrogen sorption isothermals and (d) the corresponding pore width distribution pattern of Co@C sample.

$CoCl_2 \cdot 6H_2O$ and nitrilotriacetic acid (NTA) were commercial available from Alfa Aesar and used as-received. Typically, $CoCl_2 \cdot 6H_2O$ (1.5 g) and NTA (0.6 g) were dissolved into 10 ml distilled water, under continuous stirring. After that, 30 ml isopropyl alcohol was added and further stirred for another 10 min. The final solution was transferred into a Teflon-lined autoclave and heated at 180 ^oC for 6 h. The precipitation was collected by centrifugation, washed with water and ethanol repeatedly, and dried at 60 ^oC for 12 h under vacuum. This was followed by an annealing process at 500 ^oC for 2 h in Ar atmosphere.

Synthesis of MgH_2-Co@C composites

Commercial available MgH_2 (Alfa Aesar) was pre-milled for 5 h under the protection of 0.5 MPa H_2 pressure. The ball to powder weight ratio was kept as 40:1 and ball-milled at 450 rpm. The MgH_2-Co@C composites were synthesized by mixing pre-milled MgH_2 with different weight ratio of Co@C (3, 5, 10, 15 wt%). Then the mixtures were milled for another 2 h. For comparison, pure MgH_2 was milled under the identical conditions without the addition of Co@C NPs.

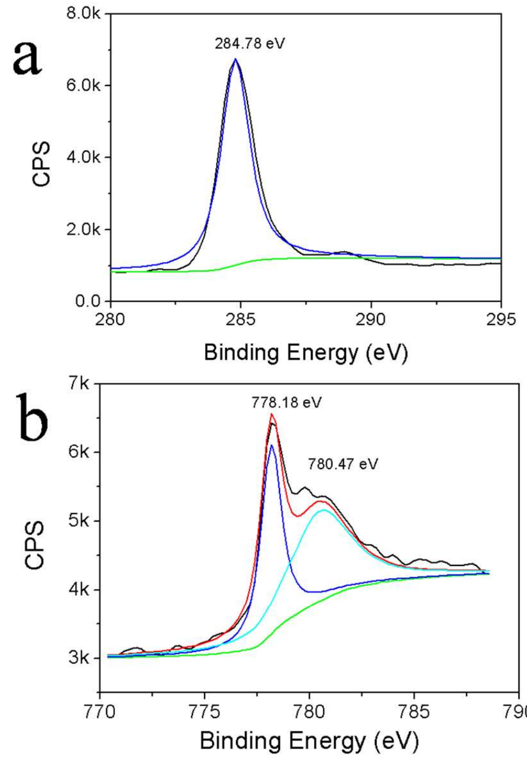

Fig.3 (a) C 1s (b) Co 2p XPS traces of the Co@C NPS.

Characterization

The structure and morphologies of as-prepared samples were characterized by X-ray diffraction (XRD, Rigaku D-Max-2500, Cu Kα radiation), Raman spectrometer (Renishaw inVia, excitation 514.5 nm), nitrogen adsorption and desorption isotherms (NOVA 2200e, Quantachrome), scanning electron microscopy (SEM JEOL JSM7500), transmission electron microscopy (TEM), scanning transmission electron microscopy (STEM), selected area electron diffraction (SAED), and high resolution transmission electron microscopy (HRTEM) on JEOL JEM-2010FEF, X-ray photoelectron spectrometer (XPS, PHI 50000 Versaprobe, ULVAC PHI). The chemical composites of the as-prepared Co@C sample were determined by inductively coupled plasma optical emissionspectrometry (ICP-OES, ICP-9000).

The dehydrogenation properties of MgH_2-Co@C composites were investigated by temperature-programmed desorption system (TPD, PX200) and differential scanning calorimetry (DSC, Q20P, TA). The isothermal desorption kinetics were performed on a home-made Sievert's instruments under the initial pressure of 0-0.05 MPa hydrogen.

Results and Discussion

Structural and morphology characterization

The core-shell structure of as-synthesized Co@C was determined by TEM (Fig 1a and 1b). Clearly, the Co@C NPs were self-assembled into a rod-like structure, which was about 100 nm in width. The SAED image (insert Fig 1a) implied that the as-synthesized Co@C had a polycrystalline nature. The rectangular

Journal of Materials Chemistry A Accepted Manuscript

This journal is © The Royal Society of Chemistry [year]

Cite this: DOI: 10.1039/c0xx00000x

www.rsc.org/xxxxxx

ARTICLE TYPE

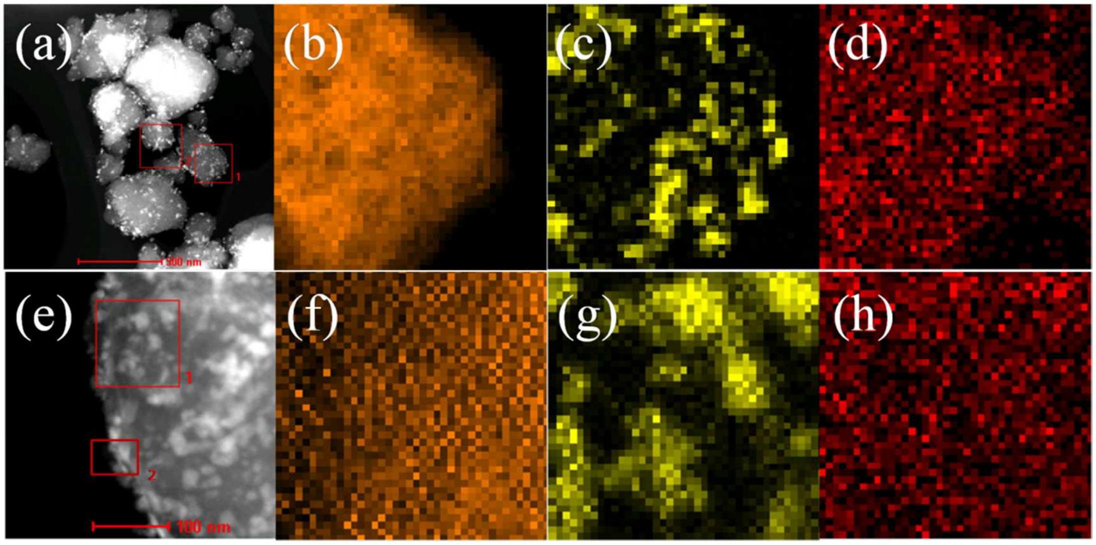

Fig. 4 Representative STEM images of the MgH_2-10%Co@C samples (a-d) as-milled, (e-f) after dehydrogenated. Mg, Co and C elements mapping are in brown, yellow and red, respectively.

region in Fig 1a was selected for the HRTEM investigation. As shown in Fig 1b, the lattice space of 2.05 Å and 1.76 Å, in the center, were referred to the (111) and (200) planes of cubic Co metal. The d-space of 3.27 Å, in the edge, was in consistence with the (002) plane of amorphous carbon. In other words, the central Co was served as core and the arrows in Fig 1b were pointed to the amorphous carbon shell. Obviously, the 3 nm amorphous carbon was uniformly surrounded on the surface of 11 nm metallic Co core. The unique morphology of core-shell Co@C was further studied by SEM, which was given in Fig 1c and 1d. The irregular rod-like structure of Co@C (Fig. 1c) was in consistence with the TEM results. Fig 1d showed that the rod-like structure was further composed of numerous ultra fine Co@C NPs.

XRD instrument was used to investigate the structure of as-synthesized Co@C NPs. As shown in Fig 2a, the broad peak centered at 25^{o} can be ascribed to the typical amorphous C (002) plane. The peaks at 44.1^{o}, 51.7^{o} and 76.0^{o} were the (111), (200) and (220) planes of the cubic Co (JCPDS card No. 89-4307), respectively. The subdued diffraction peaks of Co were due to the coated carbon shell. Thus, the core-shell structure of Co@C was further confirmed. The Co element content was obtained by ICP, which was 80.0 % in the as-synthesized Co@C.

As an important approach to demonstrate the carbon state, Raman spectrum was shown in Fig 2b. Herein, the Gaussian-Lorentzian fits were used to better illustrate the intensity, position and area of each bond. The peaks at 1355 cm^{-1} and 1589 cm^{-1} were corresponded to the D and G band, respectively. Generally, the D band was activated by the structural defects and disorders. So the D bond did not observed in highly crystalline graphite. The G bond was associated with E_{2g} phonons at Brillouin zone and can be used to investigate the graphitization. The intensity ratio of I_D/I_G in Co@C was 0.81, much higher than that of totally graphitized carbon.[23, 24] Therefore, the as-synthesized carbon shell was in amorphous state and contained plenty of defects and disordered structure.

The specific surface area and pore size distribution of Co@C were determined by nitrogen sorption isothermals, the results were shown in Fig 2c-d. The Brunauer-Emmett-Teller (BET) area of the synthesized Co@C was calculated to be 112.6 m^2 g^{-1}. Generally, the large surface area can effectively prevent the aggregation of particles and provide a more intimate reaction between catalyst and MgH_2. The pore size distribution showed a typical porous type and the mean pore size was 4.8 nm. Due to the porous structure of Co@C NPs, they can react with MgH_2 and hydrogen both on their surface and in the bulk of materials.

XPS was used to investigate the surface electrons escape of Co@C. It was clearly shown in Fig 3a that the C 1s had a main peak at 284.78 eV, which was assigned to the carbon-carbon bonds. For the Co 2p curve (Fig 3b) the peak at 778.18 eV was the metallic state of Co $2p_{3/2}$. The shoulder peak centered at 780.47 eV was caused by the surface oxidation of Co atoms.

The representative STEM pictures of the as-milled and after dehydrogenated MgH_2-10%Co@C sample were illustrated in Fig 4. Clearly, the rod-like structure of Co@C was broken during the ball-milling, but its core-shell structure was preserved and evenly distributed on the base of MgH_2/Mg during the sorption. After the dehydrogenation, both Co and C were well dispersed on the surface of Mg element. More importantly, the existence of well dispersed C can act as excellent heat exchanger during the sorption, which was good for the thermal manage of MgH_2.

Dehydrogenation performances of MgH_2-Co@C composites

In order to study the enhanced effects of core-shell Co@C on the

Journal of Materials Chemistry A Accepted Manuscript

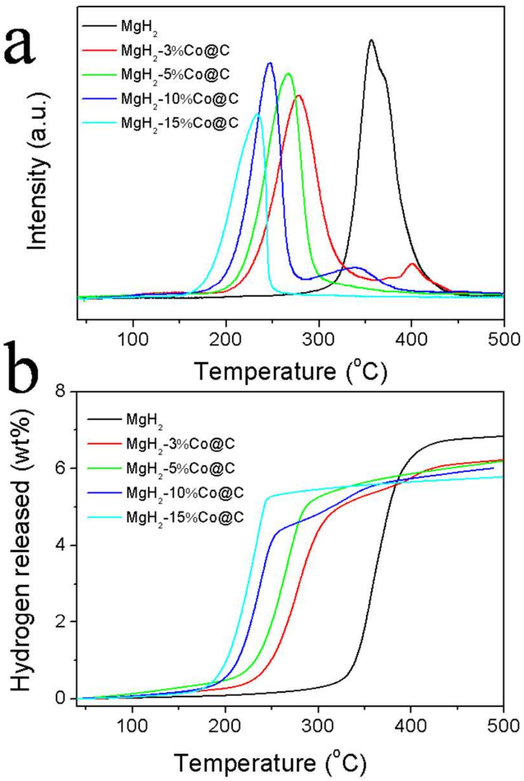

Fig.5 (a) Thermal desorption curves and (b) the corresponding hydrogen desorption patterns of as-prepared pure MgH_2 and 3 wt%, 5 wt%, 10 wt%, 15 wt% Co@C doped MgH_2 samples. Heating at 2 °C min^{-1} under Ar atmosphere

Table 1 Onset dehydrogenation temperature and the released capacity of hydrogen for as-milled samples.

Sample Name	Onset Temperature (°C)	H_2 Capacity (wt%)
MgH_2	301	6.84
MgH_2-3%Co@C	200	6.25
MgH_2-5%Co@C	185	6.20
MgH_2-10%Co@C	168	6.00
MgH_2-15%Co@C	143	5.78

dehydrogenation performances of MgH_2, the TPD investigations were carried out. Fig 5a showed that the dehydrogenation of MgH_2 was a one-step process. The visible shoulder peaks were due to the bimodal particles phenomenon.[23] Pure MgH_2 started to release hydrogen at about 301 °C, which was very high for applications. However, the onset dehydrogenation temperature of MgH_2 was significantly decreased with the addition of core-shell Co@C. Even the 3 wt% Co@C doped MgH_2 sample began to release hydrogen at a much lower temperature of 200 °C, about 101 °C decreased than that of pure MgH_2. This downward trend was more obvious with the increasing amount of Co@C. The detailed information about the operating temperature was listed in Table 1. The significantly decreased operating temperature of MgH_2 indicated that core-shell Co@C NPs can obviously improve the desorption properties of MgH_2, which was superior

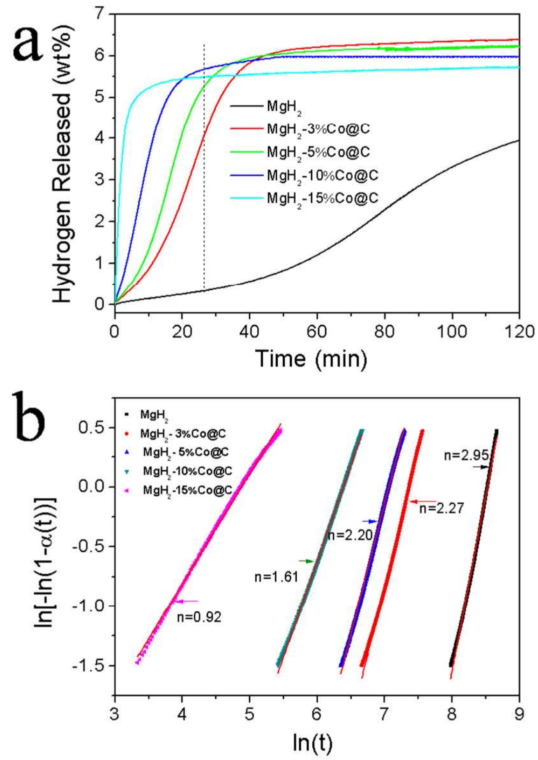

Fig.6 (a) Isothermal dehydrogenation curves of the pure MgH_2, MgH_2-3%Co@C, MgH_2-5%Co@C, MgH_2-10%Co@C and MgH_2-15%Co@C composites at 300 °C and (b) their JMA fitting plots.

than nano-Co,[7] carbon,[24, 25] and MWCNT/Co.[26]

The quantitative dehydrogenation capacities of MgH_2-Co@C compositions were calculated and shown in Fig 5b. With the increasing amount of Co@C, MgH_2 was able to desorb hydrogen at lower temperature, unfortunately, the dehydrogenation capacity of MgH_2 was also gradually decreased. As shown in Table 1, when heated to 500 °C about 6.84 wt% hydrogen was released from pure MgH_2. And this value was decreased to 6.25 wt% for MgH_2-3%Co@C, 6.20 wt% for the MgH_2-5%Co@C, 6.00 wt% for the MgH_2-10%Co@C, and finally to 5.78 wt% for the MgH_2-15%Co@C sample. The decreased capacity was caused by the high amount of additives.

Isothermal desorption experiments can clearly illustrate the dehydrogenation kinetics, so the isothermal desorption patterns were analysed and presented in Fig 6. Fig 6a showed that core-shell Co@C had positive effects in accelerating the dehydrogenation kinetics of MgH_2. Upon increasing the additive amount of Co@C, the desorption rate of MgH_2 was also increased. Especially, the MgH_2-15%Co@C sample released about 5.42 wt% hydrogen within 10 min. When heated for 25 min, the MgH_2-10%Co@C sample liberated the highest hydrogen value of 5.8 wt%. At the same time, about 5.51, 5.23 and 4.12 wt% hydrogen was released from MgH_2-15%Co@C, MgH_2-5%Co@C and MgH_2-3%Co@C, respectively. No visible hydrogen was released from pure MgH_2. The total desorption capacity showed a modest shift to the lower value with the increasing weight ratio of Co@C composites, from 6.24 wt% for

Journal of Materials Chemistry A Accepted Manuscript

This journal is © The Royal Society of Chemistry [year]

MgH_2-3%Co@C to 5.78

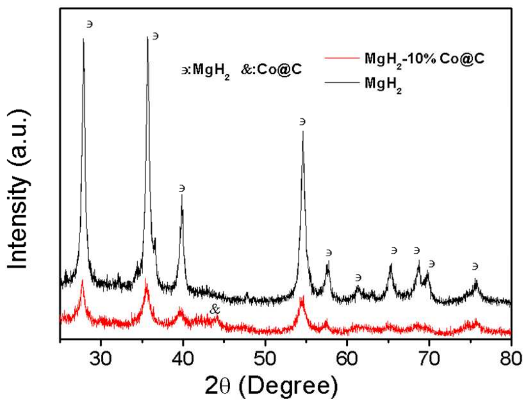

Fig.7 XRD images of the as-milled pure MgH_2 and MgH_2-10%Co@C samples.

Table 2 Representative cell parameters and grain size of the as-milled pure MgH_2 and MgH_2-10%Co@C samples.

Sample Name	Lattice Parameters (Å)		Grain Size (nm)
	a=b	c	
MgH_2	4.52	3.02	11.6
MgH_2-10%Co@C	4.51	3.01	8.70

wt% for MgH_2-15%Co@C sample. This trend was agreed with the TPD results. However, the pure MgH_2 only released about 3.8 wt% hydrogen during the test, caused by its high operating temperature.

The Johnson-Mehl-Avrami (JMA) equation is widely used to study the nucleation mechanism of solid-state reaction.[27] Generally, the JMA equation is expressed as below:

$$\ln\left[-\ln\left(1-\alpha\left(t\right)\right)\right] = n\ln\left(t\right)+n\ln\left(k\right) \tag{2}$$

Here *t* is the reaction time, *α(t)* is the dehydrogenated fraction at time *t*, *k* is the phase transformation constant, *n* is the Avrami exponent that related to the dimensionality of MgH_2/Mg transformational mechanism. Clearly, when *α(t)* varied from 0.2 to 0.8 the ln[-ln(1-α(t))] showed a straight line against ln(t). So JMA was well fitted to investigate the desorption mechanism of pure MgH_2 and MgH_2-Co@C composites. Interestingly, the Avrami exponent *n* was shifted from 2.95 for the pure MgH_2 to 2.27 and 2.20 for the MgH_2-3%Co@C and MgH_2-5%Co@C composites, continuously to 1.61 for the MgH_2-10%Co@C sample, finally to 0.92 for the MgH_2-15%Co@C sample. It was well known that different values of *n* illustrated different types of nucleation and growth mechanism. For pure MgH_2 *n* was close to 3 (2.95), so the dehydrogenation of MgH_2 was a three-dimensional growth with increased nucleation rate.[28] After the addition of 3 and 5 wt% Co@C, *n* was close to 2 (2.27 or 2.20), indicated that the dehydrogenation was a two-dimensional nucleation and growth mechanism.[29] For the MgH_2-10%Co@C sample *n* was 1.61 close to 1.5, so it was a three dimensional growth with zero nucleation growth.[30] As the doping content of Co@C increased to 15 wt%, *n* was decreased to about 1 (0.92)

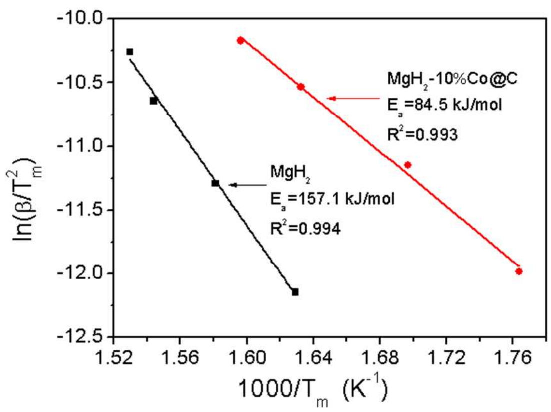

Fig.8 E_a of the as-prepared pure MgH_2 and MgH_2-10%Co@C composites, obtained by Kissinger method at the heating rate of 2, 5, 10, 15 °C min^{-1}.

which was nucleation and growth along one-dimensional dislocation lines.[31, 32] Generally, hydrogen was more easily to diffuse along lower-dimensional defects. The different nucleation and growth types of MgH_2-Co@C composites can explain the enhanced desorption kinetics of Co@C doped MgH_2 samples.

Catalytic mechanism

It was well known that the amorphous carbon shell not only made contribution to the enhanced conductivity of heat but also buffered the volume change of Co and maintained its core-shell structure during the sorption. Moreover, the existence of irregular defects in the carbon shell provided more channels and active sites for the hydrogen diffusion. At the same time, the central Co had an almost full d-band electron structure. The spin-splitting of Co-d electron made the E_g narrower than in pure MgH_2 and lead to a super structural stability of compound.[8] The unique electronic structure of Co can form a Co-H transition-state intermediate with hydrogen, which was stronger than Mg-H bond and further lead to a destabilization effects on MgH_2. Herein, the dialed catalytic mechanism of Co@C on MgH_2 was also proposed.

Taking both the operating temperature and the desorption capacity into consideration, the representative MgH_2-10%Co@C sample was selected to further study the catalytic mechanism of core-shell Co@C. The XRD patterns of pure MgH_2 and MgH_2-10%Co@C were shown in Fig 7. All the as-milled samples showed main phase of MgH_2 (JCPDS card No. 12-697), indicated that MgH_2 was well maintained during the ball-milling. For the MgH_2-10%Co@C sample the diffraction peak at 44.1° was assigned to the (111) plane of Co@C. So Co@C was survived during the synthesis procedure. Besides, the diffraction peaks of MgH_2-10%Co@C were broaden and weaken. Table 2 showed that the lattice parameter of as-milled pure MgH_2 was a=b=4.52 Å and c=3.02 Å, which was agreed with the standard value of tetragonal MgH_2. For the MgH_2-10%Co@C sample the lattice parameter was slightly decreased to a lower value of a=b=4.51 Å and c=3.01 Å. This demonstrated that Co@C may cause more

Journal of Materials Chemistry A Accepted Manuscript

metal associated defects in the MgH_2 structure, which played crucial roles in atomic transport. The grain size was 11.6 nm for pure MgH_2 and 8.70 nm for the MgH_2-10%Co@C sample,

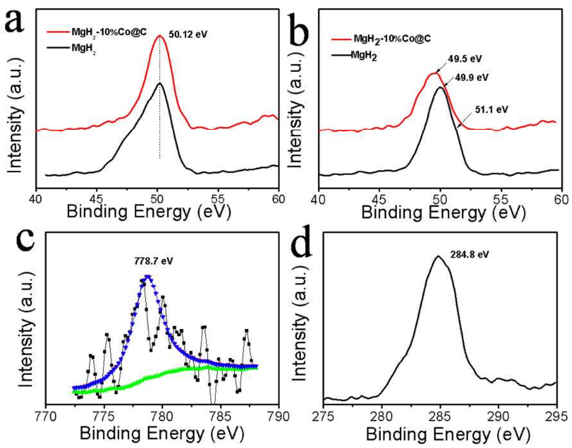

Fig.9 XPS spectra of (a) as-milled and (b) after dehydrogenated Mg 2p peaks. (c) Co 2p and (d) C 1s patterns of the dehydrogenated MgH_2-10%Co@C sample.

determined by the Scherrer equation. The smaller size of MgH_2-10%Co@C sample can partial explain the subdued MgH_2 peaks in the XRD curves. It was known that the reaction kinetics was enhanced with the decreased particle size, due to the larger surface to volume ratio and shorter solid-state diffusion distance for hydrogen.

The significantly promoted hydrogen storage properties of MgH_2 may be caused by the thermodynamics or/and kinetics modification. Here, the kinetics modification seemed to be more possible in this particle size distribution (11.6-8.7 nm). As an important factor of the kinetics, apparent activation energy (E_a) can vividly illustrate the energy barrier for the dehydrogenation of MgH_2. So the Kissinger equation is used to determine the E_a, which was expressed as following:

$$d\left[\ln\left(\frac{\beta}{T_m^2}\right)\right] / d\left(\frac{1}{T_m}\right) = \frac{-E_a}{R} \qquad (3)$$

Where β is the heating rate, T_m is the peak temperature and E_a is the apparent activation energy. The non-isothermal DSC curves were used to determine the E_a of pure MgH_2 and MgH_2-10%Co@C sample. The typical DSC curves of pure MgH_2 and MgH_2-10%Co@C were shown in Fig S1. When heated at 5 ^oC min^{-1}, the peak temperature of MgH_2-10%Co@C was 316.1 ^oC, about 43.2 ^oC lower than that of pure MgH_2. The obviously decreased peak temperature further confirmed the superior catalytic effects of Co@C. The data used to calculate the E_a of samples was listed in Table S1. Fig 8 showed that E_a for the MgH_2-10%Co@C composites was 84.5 kJ mol^{-1}, which was quite favorable than that of pure MgH_2 (157.1 kJ mol^{-1}) and other previous reported values.[7, 33-35] The obviously decreased E_a implied that the enhanced kinetics of MgH_2-10%Co@C sample was caused by the decreased energy barrier during the desorption reaction.

Fig 9 showed the XPS spectra of as-synthesized and after dehydrogenated pure MgH_2 and MgH_2-10%Co@C composites. The magnified Mg 2p curves of as-milled samples were shown in Fig 9a. Clearly, both the pure MgH_2 and MgH_2-10%Co@C showed a strong peak centered at 50.12 eV, which was corresponded to the binding energy of MgH_2.[36] The XPS spectra of dehydrogenated Mg 2p were displayed in Fig 9b. The binding energy of MgH_2-10%Co@C sample was 49.5 eV, assigned to the metallic Mg. For pure MgH_2 the binding energy of Mg 2p was little higher, a visible shoulder peak was shown at 51.1 eV which was a mixture of divalent Mg.[37, 38] So the decomposition of pure MgH_2 was incompleted. After dehydrogenation, the Co 2p peak of MgH_2-10%Co@C sample was located at 778.7 eV, indicating the existence of metallic Co. Meanwhile, the C 1s peak, at 284.8 eV, was in consistence with the as-synthesized Co@C sample. Therefore, Co@C was survived during the dehydrogenation.

The dehydrogenated samples were further collected for XRD measurement. Fig S2 showed that the main peaks for pure MgH_2 and MgH_2-10%Co@C samples were distributed to the phase of metallic Mg. However, for pure MgH_2 there were still some visible MgH_2, which can explain its lower dehydrogenation capacity. For the MgH_2-10%Co@C sample, the diffraction peak at 44.1^o was due to the existence of Co@C.

Fig S3 showed the SEM images of pure MgH_2 and MgH_2-Co@C sample. The as-milled pure MgH_2 had a serious agglomeration phenomenon, most of the larger particles were consisted of smaller particles (rang from several to hundreds nanometer). The particles size of MgH_2 was further grow during the dehydrogenation. On the other hand, the MgH_2-10%Co@C particles were well distributed. So Co@C can effectively prevent the aggregation and particle growth of MgH_2-10%Co@C sample during the dehydrogenation.

Conclusions

In summary, the core-shell Co@C NPs were synthesized via a facile hydrothermal method. Morphology characterization indicated that the as-synthesized Co@C was about 14 nm in diameter, which was composed of 11 nm Co core and 3 nm carbon shell. The as-synthesized Co@C showed enhanced catalytic effects on the dehydrogenation performances of MgH_2. The onset dehydrogenation temperature of MgH_2 was significantly decreased with the increasing amount of Co@C catalysts. From 301 ^oC for pure MgH_2 to the lowest value of 148 ^oC for the MgH_2-15%Co@C sample. Besides, the Co@C can promote the dehydrogenation kinetics of MgH_2. Further studies showed that the enhanced dehydrogenation properties of MgH_2-Co@C composites were due the obviously decreased E_a, which were 84.5 and 157.1 kJ mol^{-1} for MgH_2-10%Co@C and pure MgH_2. Theoretical modeling of the experimental data indicated that the dehydrogenation of MgH_2 proceeded through lower-dimensional growth after the addition of core-shell Co@C.

Acknowledgement

This work is gratefully acknowledge the financial support received from MOST projects (2010CB631303, 2012AA051901), NSFC (5117108), 111Project (B12015) and MOE ((IRT-13R30)).

.

Journal of Materials Chemistry A Accepted Manuscript

This journal is © The Royal Society of Chemistry [year]

Notes and references

[a] *Institute of New Energy Material Chemistry, Collaborative Innovation Center of Chemical Science and Engineering (Tianjin), Key Laboratory of Advanced Energy Materials Chemistry (MOE), Nankai University, Tianjin 300071, P. R. China. Fax: +86 22 23503639; Tel: +86 22 23503639; E-mail: wangyj@nankai.edu.cn.*

† Electronic Supplementary Information (ESI) available: See DOI: 10.1039/b000000x/

1. M. Dresselhaus and I. Thomas, *Nature*, 2001, **414**, 332-337.
2. L. Schlapbach and A. Züttel, *Nature*, 2001, **414**, 353-358.
3. A. F. Dalebrook, W. Gan, M. Grasemann, S. Moret and G. Laurenczy, *Chem Commun (Camb)*, 2013, **49**, 8735-8751.
4. R. Bardhan, A. M. Ruminski, A. Brand and J. J. Urban, *Energy Environ. Sci.*, 2011, **4**, 4882.
5. Y. S. Au, M. K. Obbink, S. Srinivasan, P. C. M. M. Magusin, K. P. de Jong and P. E. de Jongh, *Adv. Funct. Mater.*, **DOI**:10.1002/adfm.201304060.
6. J. Cui, H. Wang, J. Liu, L. Ouyang, Q. Zhang, D. Sun, X. Yao and M. Zhu, *J. Mater. Chem. A*, 2013, **1**, 5603-5611.
7. N. Hanada, T. Ichikawa and H. Fujii, *J. Phys. Chem. B*, 2005, **109**, 7188-7194.
8. N. Novakovic, J. G. Novakovic, L. Matovic, M. Manasijevic, I. Radisavljevic, B. P. Mamula and N. Ivanovic, *Int. J. Hydrogen Energy*, 2010, **35**, 598-608.
9. J. Cui, J. Liu, H. Wang, L. Ouyang, D. Sun, m. zhu and X. Yao, *J. Mater. Chem. A*, **DOI:** 10.1039/C4TA00221K.
10. M. G. Verón, H. Troiani and F. C. Gennari, *Carbon*, 2011, **49**, 2413-2423.
11. J. Mao, Z. Guo, X. Yu, H. Liu, Z. Wu and J. Ni, *Int. J. Hydrogen Energy*, 2010, **35**, 4569-4575.
12. M. G. Verón, A. M. Condó and F. C. Gennari, *Int. J. Hydrogen Energy*, 2013, **38**, 973-981.
13. C. Zhu and T. Akiyama, *Cryst. Growth. Des.*, 2012, **12**, 4043-4052.
14. X. Wang, J. Zhuang, Q. Peng and Y. Li, *Nature*, 2005, **437**, 121-124.
15. C. An, G. Liu, L. Li, Y. Wang, C. Chen, Y. Wang, L.-F. Jiao and H. Yuan, *Nanoscale*, 2014,**6**, 3223-3230.
16. M. L. Christian and K. F. Aguey-Zinsou, *ACS Nano*, 2012, **6**, 7739-7751.
17. H. Liu and G. Wang, *J. Mater. Chem. A*, **DOI:** 10.1039/C4TA01544D.
18. F. Qiu, L. Li, G. Liu, C. Xu, C. An, Y. Xu, Y. Wang, Y. Huang, C. Chen, L. Jiao and H. Yuan, *Chem-Asian J*, 2014, **9**, 487-493.
19. F. Qiu, Y. Dai, L. Li, C. Xu, Y. Huang, C. Chen, Y. Wang, L. Jiao and H. Yuan, *Int. J. Hydrogen Energy*, 2014, **39**, 436-441.
20. F. Qiu, G. Liu, L. Li, Y. Wang, C. Xu, C. An, C. Chen, Y. Xu, Y. Huang, Y. Wang, L. Jiao and H. Yuan, *Chem.–Eur. J.*, 2014, **20**, 505-509.
21. X. Wu, H. Niu, S. Fu, J. Song, C. Mao, S. Zhang, D. Zhang and C. Chen, *J. Mater. Chem. A*, 2014,**2**, 6790-6795.
22. C. An, Y. Wang, Y. Xu, Y. Wang, Y. Huang, L. Jiao and H. Yuan, ACS *App. Mater. Interfaces*, 2014, **6**, 3863-3869.
23. C. X. Shang and Z. X. Guo, *J. Power Sources*, 2004, **129**, 73-80.
24. C. Z. Wu, P. Wang, X. Yao, C. Liu, D. M. Chen, G. Q. Lu and H. M. Cheng, *J. Alloy Compd.*, 2006, **420**, 278-282.
25. C. Z. Wu, P. Wang, X. Yao, C. Liu, D. M. Chen, G. Q. Lu and H. M. Cheng, *J. Alloy Compd.*, 2006, **414**, 259-264.
26. M. G. Veron, H. Troiani and F. C. Gennari, *Carbon*, 2011, **49**, 2413-2423.
27. J. W. Christian, The Theory of Transformations in Metals and Alloys, *2nd edn., Pergamon*, 1975, New York.
28. K. L. Sahoo, A. K. Panda, S. Das and V. Rao, *Mater.s Lett.*, 2004, **58**, 316-320.
29. G. Barkhordarian, T. Klassen and R. Bormann, *J. Alloy Compd.*, 2006, **407**, 249-255.
30. C. Wu, P. Wang, X. Yao, C. Liu, D. Chen, G. Q. Lu and H. Cheng, *.J. Phys. Chem. B*, 2005, **109**, 22217-22221.
31. K.-J. Jeon, H. R. Moon, A. M. Ruminski, B. Jiang, C. Kisielowski, R. Bardhan and J. J. Urban, *Nature mater.*, 2011, **10**, 286-290.
32. Y. Liu, Y. Pang, X. Zhang, Y. Zhou, M. Gao and H. Pan, *Int. J. Hydrogen Energy*, 2012, **37**, 18148-18154.
33. Y. Jia, S. Han, W. Zhang, X. Zhao, P. Sun, Y. Liu, H. Shi and J. Wang, *Int. J. Hydrogen Energy*, 2013, **38**, 2352-2356.
34. H. Liu, X. Wang, Y. Liu, Z. Dong, G. Cao, S. Li and M. Yan, *J. Mater. Chem. A*, 2013, **1**, 12527-12535.
35. Z. Zhao-Karger, J. Hu, A. Roth, D. Wang, C. Kubel, W. Lohstroh and M. Fichtner, *Chem. Commun.*, 2010, **46**, 8353-8355.
36. S. Gupta, I. Z. Hlova, T. Kobayashi, R. V. Denys, F. Chen, I. Y. Zavaliy, M. Pruski and V. K. Pecharsky, *Chem Commun (Camb)*, 2013, **49**, 828-830.
37. K. S. Jung, D. H. Kim, E. Y. Lee and K. S. Lee, *Catal. Today*, 2007, **120**, 270-275.
38. O. Friedrichs, L. Kolodziejczyk, J. C. Sánchez-López, C. López-Cartés and A. Fernández, *J. Alloy Compd.*, 2007, **434-435**, 721-724.

Journal of Materials Chemistry A Accepted Manuscript

Journal of Materials Chemistry A Accepted Manuscript

Graphical Abstract

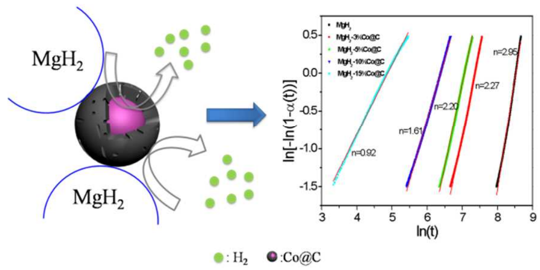

Core-shell Co@C shows excellent catalytic effects on MgH_2. JMA modeling find that desorption of MgH_2 gradually happens along lower-dimension with increase of Co@C.